# Generation of recombinant lymphocytic choriomeningitis viruses with trisegmented genomes stably expressing two additional genes of interest

**Sebastien F. Emonet, Lucile Garidou, Dorian B. McGavern, and Juan C. de la Torre[1]**

Department of Immunology and Microbial Science, The Scripps Research Institute, 10550 North Torrey Pines Road, La Jolla, CA 92037

Communicated by Michael B. A. Oldstone, The Scripps Research Institute, La Jolla, CA, January 6, 2009 (received for review November 12, 2008)

**Several arenaviruses cause hemorrhagic fever disease in humans for which no licensed vaccines are available and current therapeutic intervention is limited to the off-label use of the wide-spectrum antiviral ribavirin. However, the prototypic arenavirus lymphocytic choriomeningitis virus (LCMV) has proven to be a Rosetta stone for the investigation of virus–host interactions. Arenaviruses have a bisegmented negative-strand RNA genome. The S segment encodes for the virus nucleoprotein and glycoprotein, whereas the L segment encodes for the virus polymerase (L) and Z protein. The ability to generate recombinant LCMV (rLCMV) expressing additional foreign genes of interest would open novel avenues for the study of virus–host interactions and the development of novel vaccine strategies and high-throughput screens to identify antiarenaviral molecules. To this end, we have developed a trisegmented (1L + 2S) rLCMV-based approach (r3LCMV). Each of the two S segments in r3LCMV was altered to replace one of the viral genes by a gene of interest. All r3LCMVs examined expressing different reported genes were stable both genetically and phenotypically and exhibited wild-type growth properties in cultured cells. Reporter gene expression in r3LCMV-infected cells provided an accurate surrogate of levels of virus multiplication. Notably, some r3LCMVs displayed highly attenuated virulence in mice but induced protective immunity against a subsequent lethal challenge with wild-type LCMV, supporting the potential development of r3LCMV-based vaccines.**

antiviral screen | reverse genetic | viral attenuation

Arenaviruses merit significant interest both as tractable experimental model systems to study acute and persistent viral infections and as clinically important human pathogens (1–3). Thus, the prototypic arenavirus lymphocytic choriomeningitis virus (LCMV) has proven to be a superb workhorse in the field of virology and immunology (1). However, several arenaviruses cause hemorrhagic fever (HF) disease in humans, associated with high morbidity and mortality (2, 3). The Old World arenavirus Lassa virus (LASV) poses the highest public health concern among HF arenaviruses. LASV is estimated to infect several hundred thousand individuals yearly in its endemic region of West Africa, resulting in a high number of Lassa fever disease cases (2). Likewise, several New World arenaviruses, chiefly Junin virus, cause viral HF disease (3). Moreover, evidence indicates that the worldwide distributed LCMV is a neglected human pathogen of clinical significance (4) and poses a special threat to immunocompromised individuals (5, 6).

Public health concerns posed by human pathogenic arenaviruses are aggravated by the lack of licensed vaccines and current therapy being limited to the use of the nucleoside analog ribavirin (Rib) that can cause significant side effects and requires an early and i.v. administration for optimal efficacy (3). Therefore, it is important to develop novel effective antiarenaviral drugs and vaccines, tasks that would be facilitated by a detailed understanding of the arenavirus molecular and cell biology. Recent studies have identified small molecule inhibitors of Tacaribe virus (7) and LASV (8) cell entry, but their antiviral activity in animal models of HF arenaviruses has not been examined.

Arenaviruses are enveloped viruses with a bisegmented negative-strand (NS) RNA genome (9). Each segment, L (≈7.3 kb) and S (≈3.5 kb), uses an ambisense coding strategy to direct the synthesis of two polypeptides in opposite orientations, separated by a noncoding intergenic region. The S RNA encodes the viral nucleoprotein (NP) and glycoprotein precursor (GPC) that is posttranslationally cleaved by the cellular site 1 protease to yield the two mature virion glycoproteins GP1 and GP2, which form the spikes that decorate the surface of the virion and mediate receptor recognition and cell entry (10). The L segment encodes the viral RNA-dependent RNA polymerase (or L polymerase), and a small (≈12 kDa) RING finger protein Z that is functionally the counterpart of the matrix protein found in many enveloped NS RNA viruses. Reverse genetics systems have been now developed for LCMV (11), LASV (12), and Tacaribe virus (13), which are allowing investigators to examine the *cis*-acting sequences and *trans*-acting factors that control arenavirus replication and gene expression, as well as assembly and budding (14). Moreover, infectious LCMV has been rescued from cloned cDNAs (15, 16), which has opened the possibility of examining the phenotypes of recombinant LCMV (rLCMV) with predetermined mutations in cultured cells and whole organisms.

The generation of rLCMV expressing foreign genes of interest (GOI) would open new avenues for development of vaccines and high-throughput screen (HTS) assays to identify novel antiviral drugs to combat arenaviral infections. Several strategies have been used successfully to generate recombinant segmented NS RNA expressing foreign genes; these include: (*i*) use of an internal ribosome entry site to direct cap-independent synthesis of a protein coded by an ORF located downstream within a dicistronic mRNA (17); (*ii*) use of the self-cleaving picornavirus 2A protease to generate independently the proteins coded by genes located up- and downstream from the 2A (18); and (*iii*) use of a dicistronic genomic segment with an internal promoter (19, 20). These approaches, however, were unsuccessful in the case of LCMV. As an alternative approach, we pursued the generation of rLCMV containing three genome segments: 1L and 2S. Each of the S segments was altered to replace one of the viral ORF by the ORF of a GOI. The rationale behind this approach was that the physical separation of GP and NP into two different S segments would represent a strong selective pressure to select and maintain a virus capable of packaging 1L and 2S segments. Here, we document the efficient rescue of trisegmented rLCMV (r3LCMV) that exhibited wild-type (WT) growth properties in cultured cells, as well as high genetic and phenotypic stability. However, in vivo r3LCMV exhibited attenuation but conferred complete protection against a lethal challenge with

Author contributions: S.F.E. and J.C.d.l.T. designed research; S.F.E., L.G., and J.C.d.l.T. performed research; S.F.E., L.G., D.B.M., and J.C.d.l.T. analyzed data; and S.F.E. and J.C.d.l.T. wrote the paper.

The authors declare no conflict of interest.

[1]To whom correspondence should be addressed. E-mail: juanct@scripps.edu.

This article contains supporting information online at www.pnas.org/cgi/content/full/0900088106/DCSupplemental.

MICROBIOLOGY

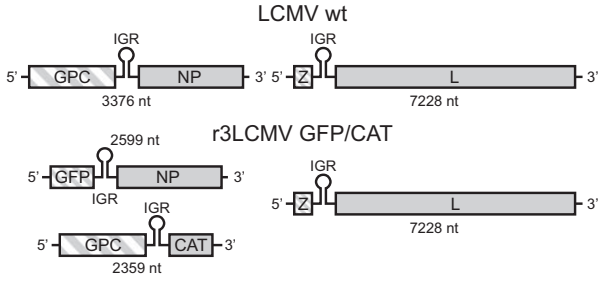


**Fig. 1.** Schematic representation of LCMV WT and r3LCMV GFP/CAT genomes. Genes in solid (NP, CAT and L) and hatched (GPC, GFP and Z) gray are transcribed from genome and antigenome templates, respectively.

LCMV WT. Characterization of r3LCMV particles showed that they were similar in size and morphology to LCMV WT. Moreover, the majority of r3LCMV infectious particles appeared to incorporate all three segments. We discuss the implications of these findings for our understanding of arenavirus biology and development of vaccines and novel HTS to identify inhibitors of arenavirus multiplication.

## Results

**Rescue of an rLCMV with a Three (2S + 1L)-Segment Genome (r3LCMV).** To determine the feasibility of rescuing viable r3LCMV, we attempted to rescue r3LCMV green fluorescent protein (GFP)/chloramphenicol acetyltransferase (CAT) containing one L and two S segments (Fig. 1). In one of the two S segments, GPC was replaced by GFP, whereas in the other S segment NP was replaced by CAT. We reasoned that a viable r3LCMV GFP/CAT will be forced to incorporate and stably maintain both S segments, which were required for production of functional GPC (GP1 + GP2) and NP. We used described reverse genetics methods (refs. 15 and 16 and *Materials and Methods*) to rescue r3LCMV GFP/CAT successfully, and as a control also a rLCMV WT. To prepare stocks from rescued viruses, we infected BHK-21 cells and collected virus-containing tissue culture supernatants at 72 h after infection (p.i.). Titers of LCMV WT and r3LCMV GFP/CAT stocks were $10^6$ and $4 \times 10^6$ focus-forming units (ffu)/mL, respectively.

**Growth Properties of r3LCMV GFP/CAT in Cultured Cells.** To compare the growth properties of r3LCMV GFP/CAT and rLCMV WT in cultured cells, we infected BHK-21 cells with each virus [multiplicity of infection (moi) = 0.1]. At different time points, virus titers in tissue culture supernatants (TCS) were determined, and cells were examined for levels of CAT and GFP expression. Both viruses exhibited similar growth properties (Fig. 2*A*). Peak titers were $2 \times 10^7$ and $2 \times 10^8$ ffu/mL for LCMV WT and r3LCMV GFP/CAT, respectively. In cells infected with r3LCMV GFP/CAT, expression of both CAT and GFP genes was readily detected, and their levels increased over time (Fig. 2 *B* and *C*).

**Genetic and Phenotypic Stability of r3LCMV.** To assess the genetic and phenotypic stability of r3LCMV, we conducted serial passages of r3LCMV GFP/CAT, and for each passage we determined virus titers in TCS and reporter gene, both CAT and GFP, expression levels. Viral titers of r3LCMV GFP/CAT and LCMV WT similarly fluctuated between $10^6$ and $10^8$ ffu/mL over 10 serial passages (Fig. 3*A*). For each passage examined (P1–P10), GFP expression was readily detected in the majority (>95%) of r3LCMV GFP/CAT-infected cells [supporting information (SI) Fig. S1]. Likewise, similar levels of CAT expression were maintained throughout the 10 passages examined (Fig. 3*B*). To evaluate the genetic stability of r3LCMV GFP/CAT, we used RNA from r3LCMV GFP/CAT-infected cells at P2 and P10 in RT-PCR assays to amplify GFP and GPC genes and determined the sequence of several independent

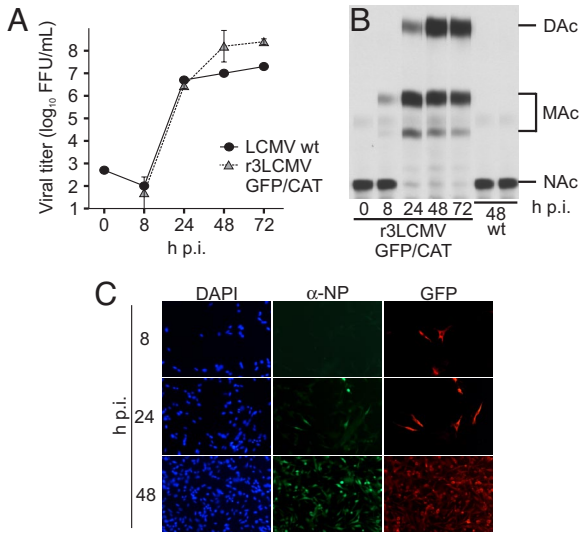


**Fig. 2.** Growth properties and foreign gene expression of r3LCMV GFP/CAT in cultured cells. BHK-21 cells were infected (moi of 0.1) either with LCMV WT or r3LCMV GFP/CAT. At the indicated time points, virus titers in supernatants were determined (*A*), and cells were either harvested for a CAT assay (*B*) or fixed and examined for NP (α-NP) and GFP expression (*C*).

clones derived from GFP and GPC RT-PCR products. We examined GPC and GFP sequences because they were located at the same position within the S RNA genomes of r3LCMV GFP/CAT, and whereas GPC sequences should be under positive selection to maintain virus infectivity, GFP sequences should not be subjected to similar selective pressures and would be able to accumulate mutations over time. Sequencing of several independent GPC and GFP clones revealed that the consensus sequences of GFP and GPC remained the same as those found in the plasmids used to rescue r3LCMV GFP/CAT (Table S1).

**Control of Virus Gene Expression in Cells Infected with r3LCMV.** Arenavirus gene expression is characterized by earlier and higher levels of NP expression compared with GPC expression in virus-infected cells. To determine whether the same temporal control and levels of virus gene expression operated in r3LCMV-infected cells, we generated r3LCMV CAT/GFP, which differed from r3LCMV GFP/CAT only on the location of GFP and CAT within the S RNA (Fig. 4*A*). Both viruses had similar growth properties in cultured cells (Fig. 4 *B* and *D*). In BHK-21 cells infected (moi = 0.01) with either r3LCMV GFP/CAT or r3LCMV CAT/GFP, both CAT and

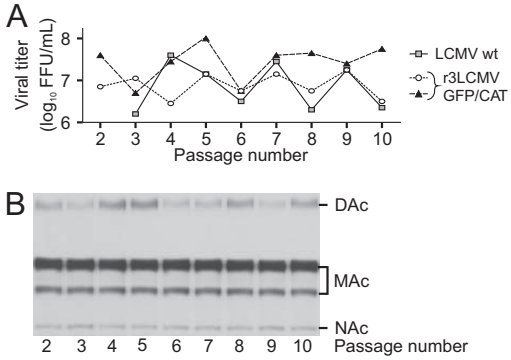


**Fig. 3.** Phenotypic stability of r3LCMV GFP/CAT during serial passages. LCMV WT and r3LCMV GFP/CAT were serially passed on BHK-21 cells. At each passage, virus titers in supernatants were determined (*A*), and r3LCMV GFP/CAT-infected cells were collected for CAT assay (*B*).

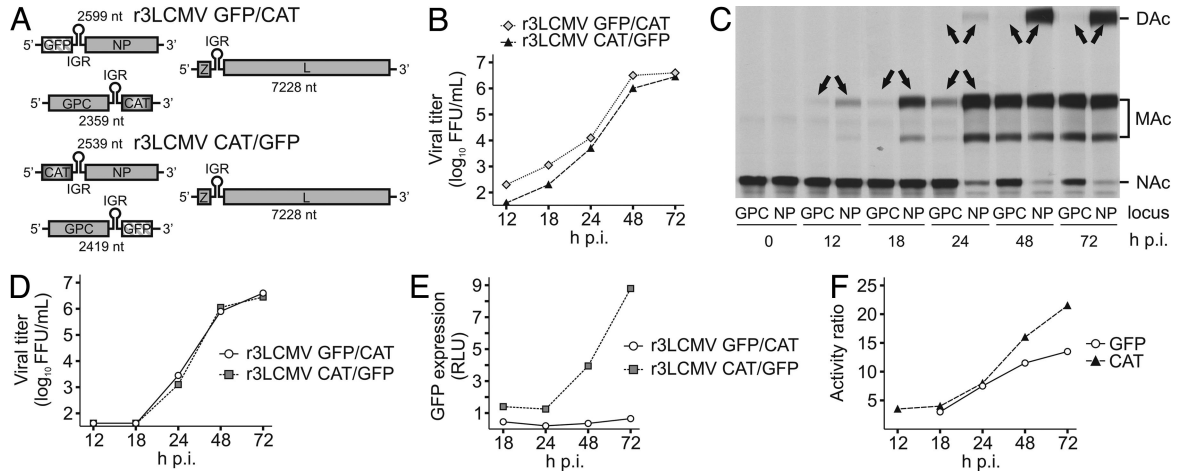


**Fig. 4.** Effect of genome location on foreign gene expression. (*A*) Two r3LCMVs (r3LCMV GFP/CAT and r3LCMV CAT/GFP) were rescued that differed only on the location within the S segment of the two foreign genes, which were inverted. (*B* and *C*) Viral titers (*B*) and CAT activity (*C*) were measured in infected (moi = 0.01) BHK-21 cells. (*D* and *E*) In an independent experiment, viral titers (*D*) and GFP expression (*E*) were determined in infected (moi = 0.01) BHK-21. (*F*) The ratio of expression levels for the same foreign gene (GFP or CAT) expressed from the NP over GPC loci was determined and normalized by the corresponding virus titers.

GFP gene expression were first detected at 12 h and 18 h p.i., respectively, regardless of their location within the S segment of r3LCMV (Fig. 4 *C* and *E*, Fig. S2). However, normalized levels of CAT activity or GFP fluorescence revealed higher levels of expression when the reporter gene was in lieu of NP than GPC (Fig. 4*F*). When CAT replaced NP, its expression levels at 18 h and 72 h p.i. were 3.9- and 21.4-fold higher than when CAT replaced GPC. In the case of the GFP gene, their differences were 2.9- and 13.4-fold.

**Characterization of r3LCMV Virions.** The ability to rescue infectious LCMV with one additional S segment raised questions about potential altered size and morphology of r3LCMV virions. To address this issue, we used electron microscopy to determine the size and morphology of virions present in TCS of cells infected with either LCMV WT or r3LCMV GFP/GFP. LCMV WT and r3LCMV GFP/GFP were similar in size (Mann–Whitney rank sum test, $P = 0.23$), with the same mean particles diameter of 62 nm (Fig. 5*A*). Likewise, both LCMV WT and r3LCMV GFP/GF particles exhibited similar morphology (Fig. 5*B*).

**Assessment of r3LCMV as a Novel Tool to Identify Antiarenaviral Molecules.** Arenaviruses are mostly noncytolytic, and recombinant arenaviruses expressing reporter genes have not been available, which has posed obstacles for the development of HTS to identify inhibitors of arenavirus multiplication. We therefore explored the potential use of a r3LCMV as a tool to develop assays amenable to HTS to identify novel candidate antiarenaviral drugs. For this we generated r3LCMV CAT/FLuc that expressed the firefly luciferase (FLuc) and CAT in lieu of NP and GPC, respectively. Both r3LCMV CAT/FLuc and WT LCMV displayed similar growth kinetics in BHK-21 cells, but r3LCMV CAT/FLuc produced slightly lower peak titers of infectious progeny (Fig. 6*A*). The kinetics and

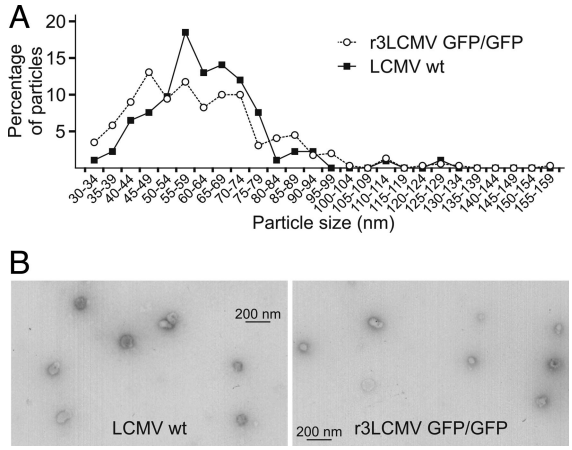


**Fig. 5.** Morphological comparison of LCMV WT and r3LCMV virions. Purified LCMV WT and r3LCMV GFP/GFP were analyzed by electron microscopy. (*A*) The diameter of particles was determined in the same horizontal axis. (*B*) Virion morphology was examined by negative staining.

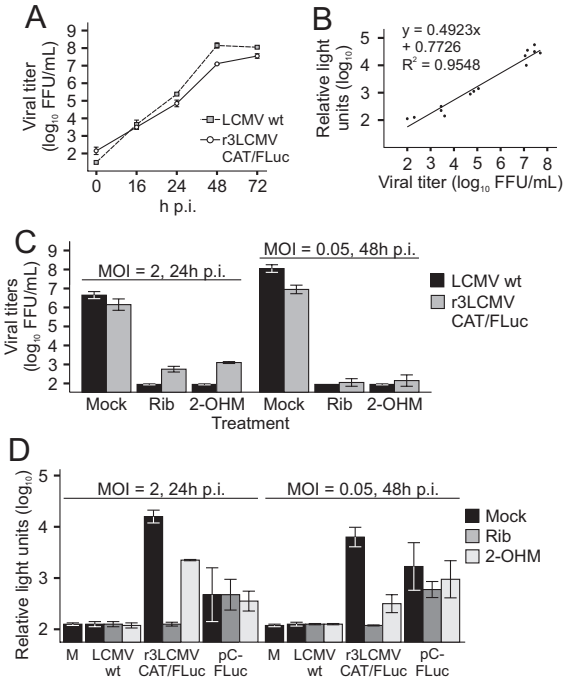


**Fig. 6.** Use of r3LCMV CAT/FLuc to identify antiarenaviral compounds. (*A*) BHK-21 cells (96-well plate) were infected (moi = 0.1) with either LCMV WT or r3LCMV CAT/FLuc and at different time points, virus titers and FLuc activity were determined. (*B*) The correlation between virus replication and FLuc expression was estimated by plotting together virus titer and FLuc activity values. (*C* and *D*) In an independent experiment, BHK-21 cells were infected at low (0.05) or high (2) moi and treated with Rib or 2-OHM or left untreated. At the indicated time, virus production (*C*) and FLuc activity (*D*) were measured.

MICROBIOLOGY

expression levels of FLuc in r3LCMV CAT/FLuc-infected cells (Fig. S3) correlated well with production of infectious virus (Fig. 6*B*). These findings supported the feasibility of using expression levels of FLuc to measure levels of virus multiplication in arenavirus-infected cells rapidly and accurately.

We next examined whether expression levels of FLuc in r3LCMV CAT/FLuc-infected cells could be used to identify candidate inhibitors of arenavirus multiplication rapidly. For this we examined, as a proof of concept, the effect of the nucleoside analog Rib and DL-2-hydroxymyristic acid (2-OHM) on FLuc expression and virus production in r3LCMV CAT/FLuc-infected cells. Rib inhibits arenavirus replication via mechanisms that have not been entirely elucidated but most likely involve the targeting of different steps of virus RNA synthesis (21). However, 2-OHM inhibits myristoylation of Z, which is required for arenavirus budding (22). Based on their mechanisms of action, we predicted that Rib would similarly inhibit production of virus progeny upon infection at low or high moi, whereas the inhibitory effect of 2-OHM would be expected to be more pronounced in infections initiated at low moi involving multiple rounds of cell infection required for virus propagation within the cell population.

To test those predictions, we infected BHK-21 cells either at low (0.05) or high (2) moi and determined FLuc expression levels and virus production at 48 h p.i. (low moi infection) or 24 h p.i. (high moi infection). Consistent with previous reports, Rib (21) and 2-OHM (22) inhibited production of infectious LCMV WT in cells infected at either high or low moi (Fig. 6*C*). As with LCMV WT, production of infectious r3LCMV CAT/FLuc was also inhibited by Rib or 2-OHM treatment, but to a slightly lesser extent when a high moi was used (Fig. 6*C*). Cells infected with r3LCMV CAT/FLuc showed levels of FLuc activity that were 54- or 127-fold over background after infection at low (48 h p.i.) or high moi (24 h p.i.), respectively (Fig. 6*D*). More importantly, in r3LCMV CAT/FLuc-infected and Rib-treated cells, levels of FLuc activity paralleled closely titers of infectious progeny (compare Fig. 6 *C* and *D*). As predicted, the effect of 2-OHM treatment on FLuc expression in r3LCMV CAT/FLuc-infected cells depended on the moi used. FLuc expression levels were reduced 7.3- and 20.9-fold after infection at high and low moi, respectively, in 2-OHM-treated cells (Fig. 6*D*).

**Characterization of r3LCMV in a Mouse Model of LCMV Infection.** To assess whether r3LCMV exhibited altered virulence in vivo, we examined the ability of r3LCMV GFP/GFP to cause lethal meningitis in mice upon intracerebral (i.c.) inoculation. In this model, i.c. inoculation of $10^3$ ffu of LCMV WT results consistently in 100% mortality within 6–8 days after inoculation (23). We used r3LCMV GFP/GFP for these studies for the following reasons: (*i*) it produces high levels of GFP expression that provided a convenient tracking method both in cell culture and in vivo; (*ii*) GFP is not found naturally in mammalian cells, and therefore its expression should not create confounding factors caused by reporter gene–cellular protein interactions during infection; and (*iii*) it exhibited WT growth properties in cultured cells (Fig. 7*A*). In contrast to our results in cultured cells, r3LCMV GFP/GFP was significantly attenuated in this model of disease as reflected by lower and delayed mortality in mice infected with r3LCMV GFP/GFP ($10^3$ ffu, i.c.) compared with LCMV WT ($10^3$ ffu, i.c.) (Fig. 7*B*). By day 8 p.i., only three of eight (37.5%) r3LCMV GFP/GFP-infected mice had died, and the remaining (five) symptomatic mice recovered and did not show noticeable clinical symptom by day 9 p.i. and thereafter. However, the use of a higher dose ($10^5$ ffu, i.c.) of r3LCMV GFP/GFP resulted in 100% lethality by day 7 p.i. ($n = 8$ mice per group) (Fig. 7*B*). To determine whether mice that survived i.c. inoculation with $10^3$ ffu r3LCMV GFP/GFP mounted a protective immune response, we challenged them at day 21 p.i. with a lethal dose ($10^3$ ffu, i.c.) of LCMV WT. All tested mice ($n = 4$) exhibited

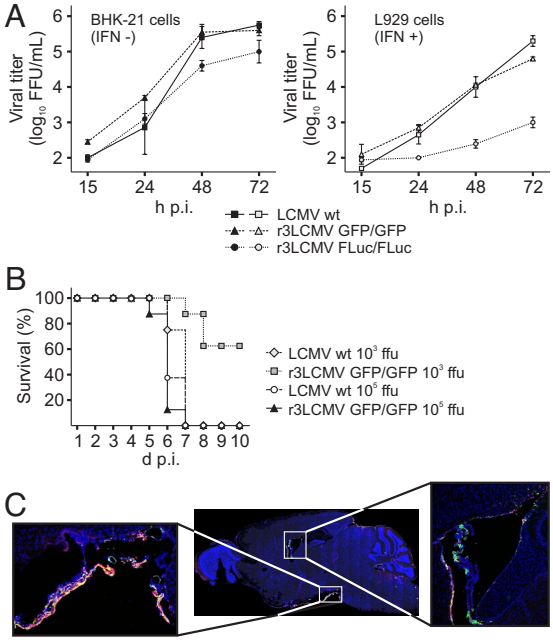


**Fig. 7.** Growth properties of r3LCMV in mice. (*A*) Growth properties in cultured cells. BHK-21 (IFN−) and L929 (IFN+) cells were infected with the indicated viruses (moi = 0.01), and at the indicated hour p.i., virus titers in supernatants were determined. (*B*) r3LCMV GFP/GFP was compared with LCMV WT in the mouse model of LCMV-induced lethal meningitis. Mice ($n = 8$) were injected i.c. with either $10^3$ or $10^5$ ffu of LCMV WT or r3LCMV GFP/GFP and checked daily for clinical symptoms and survival. (*C*) The tropism and GFP expression of r3LCMV GFP/GFP were determined in brains of mice injected (i.c.) with $10^5$ ffu at day 5 p.i.

complete protection reflected by the lack of clinical symptoms and survival after the challenge.

To determine whether r3LCMV GFP/GFP and LCMV WT exhibited the same tropism in the brain of infected mice, we inoculated (i.c.) mice ($n = 2$ per group) with $10^5$ ffu of either LCMV WT or r3LCMV GFP/GFP and collected brains at day 6 p.i., when mice were symptomatic. To determine virus distribution in brain, sagittal brain sections were examined by immunohistochemistry. Consistent with previous findings (24), LCMV WT infected mainly four areas in the brain (Fig. S4): meninges, ependyma, choroid plexus, and olfactory bulb. The r3LCMV GFP/GFP showed a similar, but more restricted, distribution (Fig. 7*C*). Cells in the ependyma, choroid plexus, and olfactory bulb were clearly infected by r3LCMV GFP/GFP, whereas infection of the meninges was patchy compared with LCMV WT. GFP expression in r3LCMV GFP/GFP-infected mice colocalized with viral antigens and was high enough to be detected without the need of any amplification (Fig. 7*C* and Fig. S4).

## Discussion

Here, we have documented the rescue of trisegmented LCMV and shown that r3LCMV has WT growth properties in cultured cells and is both genetically and phenotypically stable. Our rationale behind the strategy for the generation of r3LCMV was that the physical separation of GPC and NP into two different S segments would represent a strong selective pressure to select and maintain a virus capable of packaging 1L and 2S segments, where each of the S segments could direct expression of a GOI. We have rescued more than 10 different r3LCMCs expressing a variety of non-LCMV genes, which illustrates the robustness of this strategy to generate rLCMVs expressing additional GOI.

NS RNA viruses, including arenaviruses, have error-prone polymerases that confer them with the potential for rapid evolution (25). This, in turn, likely contributes to the often-

observed loss of foreign gene expression over time by recombinant NS RNA viruses (19, 26). Notably, rLCMV GFP/CAT displayed high both genetic and phenotypic stability. During serial passages of rLCMV GFP/CAT at low moi, no mutations were fixed within the consensus sequence of GFP. Likewise, we did not detect any truncated GFP or any other sign of genome reorganization in r3LCMV GFP/CAT.

Regulation of GOI expression by r3LCMV was similar to the one observed for bona fide viral genes in LCMV WT-infected cells. Several studies have shown higher levels of NP mRNA than GPC mRNA throughout all times examined in LCMV-infected cells (27, 28). Accordingly, CAT and GFP expression levels were higher when placed in lieu of NP than GPC (Fig. 4*B*). We observed that in r3LCMV-infected cells the ratio of NP-located to GPC-located GOI mRNA levels increased throughout the infection, whereas a previous report documented a constant 5-fold excess of NP mRNA over GPC mRNA in LCMV-infected BHK-21 cells (28). This apparent discrepancy might be the result of methodological differences, including moi used and measurement of mRNA versus protein activity. Expression levels of the same GOI depended on its location within the S genome, indicating that the control of arenavirus gene expression is determined mainly by the 5′- and 3′-noncoding regions, together with the intergenic region. Nevertheless, the regulatory mechanisms by which the arenavirus polymerase directs higher transcriptional levels of NP-located versus GPC-located genes but lower levels of antigenome versus genome RNA species remain to be determined.

LCMV WT and r3LCMV GFP/GFP exhibited similar growth properties in cultured cells (Fig. 7*A*), but r3LCMV GFP/GFP was significantly attenuated in a mouse model of LCMV-induced fatal meningitis (Fig. 7*B*). However, r3LCMV GFP/GFP exhibited the same cell tropism, although restricted spread, as LCMV WT within the mouse CNS (Fig. 7*C* and Fig. S4). We have made similar observations with several other r3LCMVs tested. The mechanisms responsible for this in vivo attenuation of r3LCMVs, despite their WT growth properties in cultured cells, are under investigation.

Reduced ffu to particle ratio may have contributed to the attenuation of r3LCMV in mice because an increased number of nonreplicating particles within the virus inoculum could result in a faster and enhanced innate immune response leading to the control of virus multiplication. In this regard, our EM studies consistently revealed higher number of r3LCMVs than LCMV WT particles for viral preparations containing the same infectious titers (ffu per mL). Nevertheless, the absence of a quantifiable reference precluded us from comparing ffu/particle ratios between samples accurately.

Our results would suggest that unlike the influenza virus (29 and references therein) but similar to bunyamwera virus (30), coding regions do not appear to play a critical role in arenavirus packaging, and either GPC or NP could be entirely replaced by a GOI without any noticeable attenuation of the r3LCMV in cell culture. The maximum number of segments that could be incorporated per arenavirus particle remains to be determined, but the total genome length appears to influence the fitness of r3LCMV. Firefly luciferase (1.6 kb) was the largest GOI we incorporated into an r3LCMV, and the rescued r3LCMV FLuc/FLuc with a total genome size of 14.1 kb (10.6 kb for the LCMV WT) was attenuated not only in vivo but also in cultured cells (Fig. 7*A*). It is plausible that the upper limit genome size that can be packaged efficiently into arenavirus virions is not far from one L plus two S segments (≈14 kb), which would explain the attenuated phenotype of r3LCMV FLuc/FLuc in cultured cells.

The mechanisms that regulate arenavirus genome packaging remain largely unknown, and only the requirement of the intergenic region to form virus-like particles has been demonstrated (14). Notably, at early times after infection at low moi with r3LCMV CAT/GFP, most (>95%) NP-positive cells also expressed GFP (Fig. S2), indicating that the majority of r3LCMV CAT/GFP infectious virions contained both (GPC-GFP and CAT-NP) S segments. There are some precedents based on both genetics (9) and structural (10, 31) analysis in support of S polyploidy within arenavirus infectious particles. Our data showed that preparations of infectious particles from LCMV WT and r3LCMV were undistinguishable either by size or shape, but we were unable to determine precisely the percentage of particles with two or three segments present within the r3LCMV population. Nevertheless, these findings suggest that production of infectious arenavirus particles containing two S and one L segments could be a very common event. Intriguingly, the L polymerase and Z proteins within the L segment exhibit higher genetic diversity than the NP and the signal peptide and GP2 portions of the GPC within the S segment (32, 33) (Fig. 8), a unique evolutionary feature among enveloped riboviruses. It is plausible that the arenavirus ability to form virions diploid for the S segment may act as a buffer against the accumulation of mutations for GPC and NP. Consequently, genes located on the S segment would be more protected against genetic drift than genes located on the L segment.

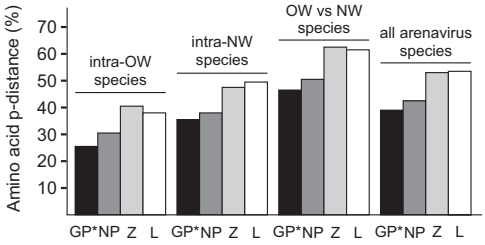


**Fig. 8.** Amino acid diversity among arenavirus proteins. The amino acid alignments used to infer phylogenetic relationships among arenavirus species (34) were used to measure the amino acid diversity by pairwise distance in different arenavirus groups. Because GP1 was too divergent to be aligned among groups, we combined the signal peptide and GP2 sequences (GP*) instead of the full GPC for this analysis.

The strategy we have developed offers new opportunities for arenavirus research, including mechanisms responsible for the control of virus gene expression and genome packaging. The generation of r3LCMVs expressing appropriate reporter genes can provide tools for the development of assays to identify novel antiviral molecules against clinically important viruses responsible of HF in humans in West Africa and South America (3). Moreover, r3LCMVs are strongly attenuated in vivo and able to express two foreign genes, which may be harnessed for the development of multivalent vaccine viruses (35). This potential is underscored by the complete protection against a lethal challenge with the LCMV WT seen in mice that had been infected with r3LCMV GFP/GFP. Likewise, confirmation that arenavirus virions often pack 2S and 1L genome segments would significantly impact our understanding of arenavirus genetics.

## Materials and Methods

**Viruses and Cells.** Vero E6 and BHK-21 cells were grown in Dulbecco's modified Eagle's medium (DMEM) (Invitrogen) containing 10% FBS. L929 cells were grown in minimum essential medium (MEM) containing 7% FBS. Media were supplemented with 2 mM L-glutamine, 100 μg/mL streptomycin, and 100 units/mL penicillin. Infected and transfected cells were maintained in a mixture (50:50) of Opti-MEM and their normal medium. Stocks of LCMV WT (Armstrong strain) and recombinant trisegmented LCM viruses were produced by infecting BHK-21 cells (moi = 0.01–0.1) and harvesting the supernatant at 72 h p.i. Virus titers (ffu) were determined by immunofocus assay (36). Briefly, 10-fold serial virus dilutions were used to infect VERO cell monolayers in a 96-well plate, and at 20 h p.i., cells were fixed by using 4% formaldehyde in PBS. After cell permeabilization by treatment with 0.3% Triton X-100 in PBS containing 3% BSA, cells were stained by using an anti-NP mouse monoclonal antibody and an Alexa Fluor 568-labeled anti-mouse second antibody (Molecular Probes). Trisegmented viruses are referred to as r3LCMV X/Y where X represents the sequence in lieu of GPC and Y the sequence in lieu of NP.

**DNA Transfection and Rescue of LCMV from Cloned cDNAs.** Virus rescue was done essentially as described (15, 16). Subconfluent BHK-21 cells ($2 \times 10^6$ cells per M6 well) were transfected for 5 h by using 2.5 $\mu$L of Lipofectamine 2000 (Invitrogen) per microgram of plasmid DNA. The mixture plasmid included 0.8 $\mu$g of pC-NP and 1 $\mu$g of pC-L, together with plasmids pol-I L (1.4 $\mu$g) and pol-I S (0.8 $\mu$g) that directed intracellular synthesis, via RNA pol-I, of the viral L and S genome RNA species. For the rescue of a r3LCMV containing 1L and 2S genome RNAs, each pol-I S (0. 8 $\mu$g) expressing the modified S segment was incorporated into the transfection mix. The vectors used to insert a GOI into the S genomic segment backbone were pol-I GPC/BbsI and pol-I BsmBI/NP. GOI were cloned via either BbsI (NP locus) or BsmBI (GPC locus) cloning sites. The BbsI site naturally found in LCMV Armstrong GPC sequence was removed by site-directed mutagenesis. Foreign genes were amplified by using the PCR Extender System (5 Prime) and primers with either BsmBI or BbsI sites, and inserted into the opened vectors.

**Foreign Gene Expression Analysis.** CAT expression was determined as described in ref. 11 and normalized to equal amounts of protein in each cell lysate, as determined by using the BCA protein assay kit (Pierce). FLuc activity was quantified by using the ONE-Glo luciferase assay system (Promega), following the manufacturer's recommendations. GFP expression was monitored by using an epifluorescence microscope. GFP expression in LCMV-infected cells was quantified by determining their green light emission. For this, infected cells were identified based on their NP expression detected by immunofocus assay, and images of a field of infected cells were collected by using constant parameters either on the red channel (anti-LCMV NP staining) or on the green channel (GFP expression). The software Photo-paint 12 (Corel) was used to define a mask based on the red color to delimit infected cells. The surface covered by the mask was then used to measure the green luminosity on the green channel by using the histogram function of the software. We also measured the light detected on the green channel on the remaining surface of the collected image (noninfected cells) to determine the light background level.

**Mice Experiments.** To assay the virulence of r3LCMV, C57/BL6 mice were inoculated i.c. with the indicated r3LCMV or LCMV WT by using either $10^3$ or $10^5$ ffu. Mice were monitored daily for clinical symptoms and survival. To determine the tropism and the in situ GFP expression of r3LCMV GFP/GFP, brains from infected mice were collected at day 5 p.i., and 6-$\mu$m sagittal sections were prepared by immunohistochemistry with antibodies against GPC (LCMV) and/or GFP. Three-color organ reconstructions to visualize the distribution of GFP (green), LCMV (red), and cell nuclei (blue) were obtained by using an immunofluorescence microscope (Axiovert S100; Carl Zeiss MicroImaging) and a 5× objective. Reconstructions were performed by using the MosaiX function in KS300 image analysis software (Carl Zeiss MicroImaging). Higher-resolution images were captured with a 5× objective and AxioVision software (Carl Zeiss MicroImaging). All experiments involving the use of mice were done according to the protocol approved by the Institutional Animal Care and Use Committee (IACUC) at The Scripps Research Institute.

**Electron Microscopy Studies.** Supernatants from infected BHK-21 were filtrated by using Amicon Ultra-15 100K columns (Millipore) for 10 min at 1,500 × *g* to concentrate virus particles. Concentrate virus samples were layered over a discontinuous sucrose gradient, consisting of two 1-mL cushions of 60% and 20% sucrose in TNE [10 mM Tris, 150 mM NaCl, 1 mM EDTA (pH 8.0)] and centrifuged at 4 °C for 2 h at 50,000 rpm in a Beckman SW60 rotor. The interphase between the 20% and 60% sucrose was collected, diluted 1/3 with TNE buffer, and centrifuged at 4 °C onto a 20% sucrose cushion for 2 h at 50,000 rpm in a Beckman SW60 rotor. The supernatant was removed, and the pellet was resuspended into 100 $\mu$L of TNE. Samples were fixed by using 2.5% (final concentration) glutaraldehyde and stained with 2% uranyl acetate before being charged onto carbon-coated grids.

**Drug Treatment.** Stock solutions (10 mM) of Rib and 2-OHM (Sigma) were prepared in Opti-MEM and ethanol, respectively. Rib and 2-OHM were used at a final concentration of 100 $\mu$M.

**RNA Preparation and Sequencing.** RNA was extracted from cells by using TRI reagent (Molecular Research Center). Reverse-transcription reaction was done with 600 ng of RNA by using the Masterscript kit (5 PRIME) and primers specific for either GFP or LCMV GPC genes. PCRs were done with the PCR Extender System (5 PRIME) with 2 $\mu$L of cDNA from the RT reaction. Amplified products were ligated into pCR 2.1 vector by using the Original TA cloning kit (Invitrogen). Ligation products were used to transform One Shot TOP10 bacteria. DNA was isolated from individual clones by using the QIAprep spin miniprep kit (Qiagen) and their sequence determined.

**ACKNOWLEDGMENTS.** We thank Dr. Malcolm Wood for his help with the electron microscope experiments. This work was supported by National Institutes of Health Grants AI-47140 and AI-065359 (to J.C.d.l.T.), AI-075298-01 (to D.B.M.), and a grant from the Burroughs Wellcome Fund (to D.B.M.). S.F.E. was supported by the Délégation Générale pour l'Armement (Convention de Subvention Grant 06.60.040.00.470.75.01). This is The Scripps Research Institute manuscript 19860 from the Department of Immunology and Microbial Science.

1. Zinkernagel RM (2002) Lymphocytic choriomeningitis virus and immunology. *Curr Top Microbiol Immunol* 263:1–5.
2. Günther S, Lenz O (2004) Lassa virus. *Crit Rev Clin Lab Sci* 41:339–390.
3. Charrel RN, de Lamballerie X (2003) Arenaviruses other than Lassa virus. *Antiviral Res* 57:89–100.
4. Barton LL (1996) Lymphocytic choriomeningitis virus: A neglected central nervous system pathogen. *Clin Infect Dis* 22:197.
5. Fischer SA, *et al.* (2006) Transmission of lymphocytic choriomeningitis virus by organ transplantation. *N Engl J Med* 354:2235–2249.
6. Palacios G, *et al.* (2008) A new arenavirus in a cluster of fatal transplant-associated diseases. *N Engl J Med* 358:991–998.
7. Bolken TC, *et al.* (2006) Identification and characterization of potent small molecule inhibitor of hemorrhagic fever New World arenaviruses. *Antiviral Res* 69:86–97.
8. Lee AM, *et al.* (2008) Unique small molecule entry inhibitors of hemorrhagic fever arenaviruses. *J Biol Chem* 283:18734–18742.
9. Meyer BJ, de la Torre JC, Southern PJ (2002) Arenaviruses: Genomic RNAs, transcription, and replication. *Curr Top Microbiol Immunol* 262:139–157.
10. Buchmeier MJ (2002) Arenaviruses: Protein structure and function. *Curr Top Microbiol Immunol* 262:159–173.
11. Lee KJ, Novella IS, Teng MN, Oldstone MB, de La Torre JC (2000) NP and L proteins of lymphocytic choriomeningitis virus (LCMV) are sufficient for efficient transcription and replication of LCMV genomic RNA analogs. *J Virol* 74:3470–3477.
12. Hass M, Gölnitz U, Müller S, Becker-Ziaja B, Günther S (2004) Replicon system for Lassa virus. *J Virol* 78:13793–13803.
13. López N, Jácamo R, Franze-Fernández MT (2001) Transcription and RNA replication of Tacaribe virus genome and antigenome analogs require N and L proteins: Z protein is an inhibitor of these processes. *J Virol* 75:12241–12251.
14. Pinschewer DD, Perez M, de la Torre JC (2005) Dual role of the lymphocytic choriomeningitis virus intergenic region in transcription termination and virus propagation. *J Virol* 79:4519–4526.
15. Sánchez AB, de la Torre JC (2006) Rescue of the prototypic arenavirus LCMV entirely from plasmid. *Virology* 350:370–380.
16. Flatz L, Bergthaler A, de la Torre JC, Pinschewer DD (2006) Recovery of an arenavirus entirely from RNA polymerase I/II-driven cDNA. *Proc Natl Acad Sci USA* 103:4663–4668.
17. García-Sastre A, Muster T, Barclay WS, Percy N, Palese P (1994) Use of a mammalian internal ribosomal entry site element for expression of a foreign protein by a transfectant influenza virus. *J Virol* 68:6254–6261.
18. Percy N, Barclay WS, García-Sastre A, Palese P (1994) Expression of a foreign protein by influenza A virus. *J Virol* 68:4486–4492.
19. Machado AV, Naffakh N, van der Werf S, Escriou N (2003) Expression of a foreign gene by stable recombinant influenza viruses harboring a dicistronic genomic segment with an internal promoter. *Virology* 313:235–249.
20. Flick R, Hobom G (1999) Transient bicistronic vRNA segments for indirect selection of recombinant influenza viruses. *Virology* 262:93–103.
21. Ruiz-Jarabo CM, Ly C, Domingo E, de la Torre JC (2003) Lethal mutagenesis of the prototypic arenavirus lymphocytic choriomeningitis virus (LCMV). *Virology* 308:37–47.
22. Perez M, Greenwald DL, de la Torre JC (2004) Myristoylation of the RING finger Z protein is essential for arenavirus budding. *J Virol* 78:11443–11448.
23. Traub E (1936) An epidemic in a mouse colony due to the virus of acute lymphocytic choriomeningitis. *J Exp Med* 63:533–546.
24. Kang SS, McGavern DB (2008) Lymphocytic choriomeningitis infection of the central nervous system. *Front Biosci* 13:4529–4543.
25. Duffy S, Shackelton LA, Holmes EC (2008) Rates of evolutionary change in viruses: Patterns and determinants. *Nat Rev Genet* 9:267–276.
26. Billecocq A, *et al.* (2008) RNA polymerase I-mediated expression of viral RNA for the rescue of infectious virulent and avirulent Rift Valley fever viruses. *Virology* 378:377–384.
27. Franze-Fernández MT, *et al.* (1987) Molecular structure and early events in the replication of Tacaribe arenavirus S RNA. *Virus Res* 7:309–324.
28. Fuller-Pace FV, Southern PJ (1988) Temporal analysis of transcription and replication during acute infection with lymphocytic choriomeningitis virus. *Virology* 162:260–263.
29. Marsh GA, Rabadán R, Levine AJ, Palese P (2008) Highly conserved regions of influenza a virus polymerase gene segments are critical for efficient viral RNA packaging. *J Virol* 82:2295–2304.
30. Kohl A, Lowen AC, Léonard VH, Elliott RM (2006) Genetic elements regulating packaging of the Bunyamwera orthobunyavirus genome. *J Gen Virol* 87:177–187.
31. Young PR, Howard CR (1983) Fine structure analysis of Pichinde virus nucleocapsids. *J Gen Virol* 64:833–842.
32. Vieth S, Torda AE, Asper M, Schmitz H, Günther S (2004) Sequence analysis of L RNA of Lassa virus. *Virology* 318:153–168.
33. Emonet S, Lemasson JJ, Gonzalez JP, de Lamballerie X, Charrel RN (2006) Phylogeny and evolution of Old World arenaviruses. *Virology* 350:251–257.
34. Charrel RN, de Lamballerie X, Emonet S (2008) Phylogeny of the genus *Arenavirus*. *Curr Opin Microbiol* 11:362–368.
35. von Messling V, Cattaneo R (2004) Toward novel vaccines and therapies based on negative-strand RNA viruses. *Curr Top Microbiol Immunol* 283:281–312.
36. Battegay M (1993) Quantification of lymphocytic choriomeningitis virus with an immunological focus assay in 24-well plates. *ALTEX* 10:6–14.